37. HISTORY OF PLIO-PLEISTOCENE CLIMATE IN THE NORTHEASTERN ATLANTIC, DEEP SEA DRILLING PROJECT HOLE 552A[1]

H. B. Zimmerman, Union College
N. J. Shackleton, Cambridge University
J. Backman, University of Stockholm
D. V. Kent, Lamont-Doherty Geological Observatory
J. G. Baldauf, U. S. Geological Survey
A. J. Kaltenback, Marathon Oil Co.
and
A. C. Morton, British Geological Survey, Keyworth[2]

ABSTRACT

DSDP Hole 552A, cored with the HPC on Hatton Drift, represents an almost complete and undisturbed sediment section spanning the late Neogene and Quaternary. Lithologic, faunal, isotopic, and paleomagnetic analyses indicate that the section represents the most complete deep sea record of climatic evolution hitherto recovered at high latitudes in the northern hemisphere. A glacial record of remarkable resolution for the late Pliocene and Pleistocene is provided by oxygen and carbon isotope ratios in benthic foraminifers. In the upper part of the section, the whole of the standard oxygen isotope record of the past million years is well preserved. The onset of ice-rafting and glacial-interglacial alternations occurs at about 2.4 m.y. ago.

INTRODUCTION

The introduction of the hydraulic piston corer (HPC) by the Deep Sea Drilling Project (DSDP) has provided, for the first time, the ability to retrieve virtually undisturbed sections of Neogene sediment from the deep ocean. In HPC Hole 552A, we obtained an almost complete record of the inception of glaciation and subsequent variation of Plio-Pleistocene climate in a high latitude region of the North Atlantic (Figs. 1, 2). In this chapter we summarize the sedimentologic, faunal, geochemical, paleomagnetic, and isotopic data generated by examination of this core.

A relatively high rate of sediment accumulation at HPC Hole 552A provided an unusual and detailed Plio-Pleistocene record with good resolution and minimal bioturbation. In contrast, relatively few conventional piston cores, such as core V28-239, contain a complete record of glacial stratigraphy because bioturbation and low rates of accumulation obscure the fine-scale resolution of detailed features of the climatic record.

In Hole 552A deposition is fashioned by the interplay of two climatically controlled processes: the influx of noncarbonate material transported primarily by ice-rafting and bottom currents and the changing production of calcareous microfossils in the surface waters (carbonate dissolution is of little importance at the water depths of this site). The section is thus characterized by a striking alternation of biogenic ooze and terrigenous muds. A uniform rate of sedimentation is certainly unlikely with so dramatic a variation in the nature of the sediments. Although depositional processes are variable, the core nevertheless exhibits a remarkably complete stratigraphic record.

METHODS

All cores from Hole 552A were extremely well preserved (see Site 552 chapter) with the exception of Core 6 (24–29 m sub-bottom). Because of severe disturbance, Core 6 was excluded from all analyses.

Total carbonate content was determined by the "Karbonate Bombe" technique (Müller and Gastner, 1971). In this procedure, a sample is powdered, weighed, and treated with 6*N* HCl in a closed cylinder. The resulting CO_2 pressure is proportional to the $CaCO_3$ content of the sample. Application of an appropriate calibration factor to the manometer reading yields percent $CaCO_3$. For sediments rich in $CaCO_3$, error is generally as low as 1%. Repeated analyses show that an accuracy of $\pm 2\%$ is obtained for samples with $CaCO_3$ content below 10%. Analyses were made on the whole sediment and on the coarse fraction (CF) after screening at 74 μm (Table 1, Fig. 3).

Following carbonate determination, the remaining acid-insoluble fraction of selected samples was examined petrographically (Morton, this volume). Cores 1 through 10 were examined for major compositional variation. A closely spaced sample set for Cores 1 and 2 was examined for the abundance of volcanic glass. A small number of samples were also analyzed for heavy mineral content, following separation from the light minerals by gravity-settling in bromoform (sp. grav. 2.80).

Organic geochemical and visual kerogen analysis was performed on selected samples covering two glacial-interglacial cycles from near the top and bottom of the section. Sedimentary organic matter was evaluated by Rock-Eval pyrolysis, determination of organic phosphorous, and pyrolysis/mass spectrometry (Figs. 4, 5). A complete description of these methodologies and results is given in Kaltenback et al. (this volume).

Diatom biostratigraphy in the Plio-Pleistocene section was established by Baldauf (this volume). Values of species abundance were based on the average number of diatom frustules observed per field of view (at least 450 fields of view per sample; 0.5 mm^2 at 500×).

[1] Roberts, D. G., Schnitker, D., et al., *Init. Repts. DSDP*, 81: Washington (U.S. Govt. Printing Office).

[2] Addresses: (Zimmerman) Union College, Schenectady, New York; (Shackleton) Godwin Laboratory for Quaternary Research, Cambridge University, Cambridge CB2.3 RS, United Kingdom; (Backman) Department of Geology, University of Stockholm, Stockholm, S-106 91, Sweden; (Kent) Lamont-Doherty Geological Observatory, Palisades, NY 10964; (Baldauf) U.S. Geological Survey, Menlo Park, CA 94025; (Kaltenback) Marathon Oil Company, Denver Research Center, Littleton, CO 80160; (Morton), British Geological Survey, Keyworth NG12 5GG, United Kingdom.

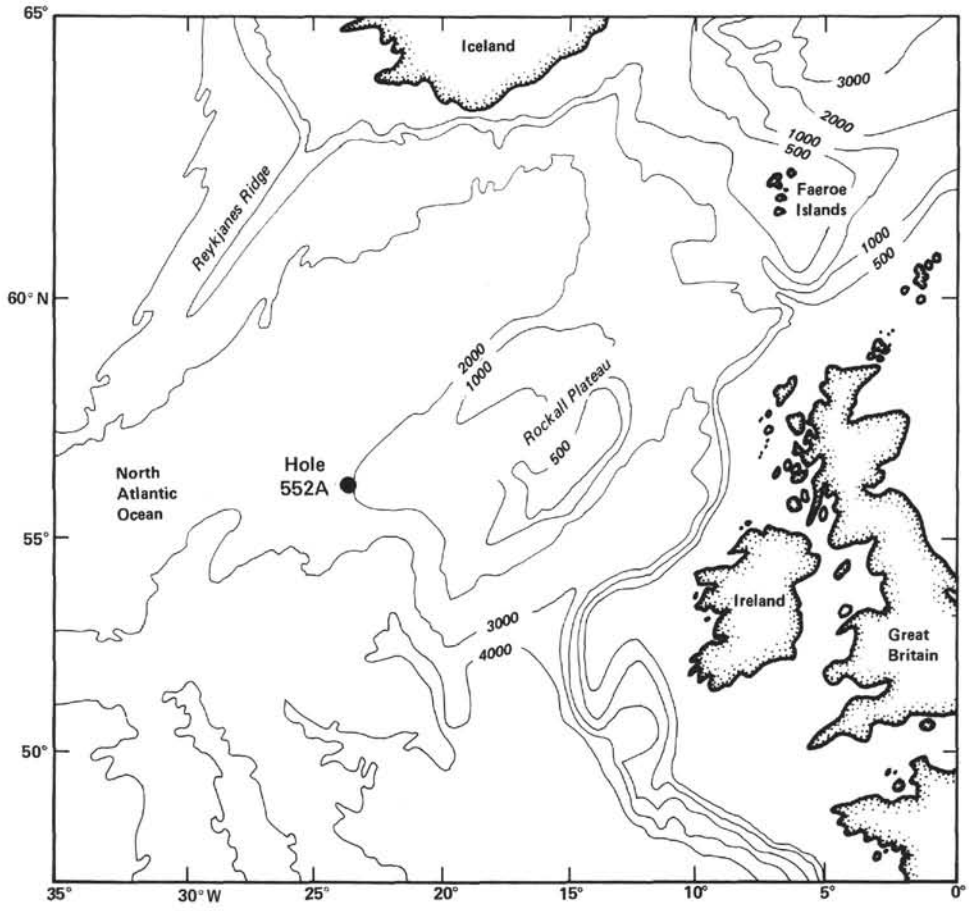

Figure 1. Location map for Hole 552A (56°02.56'N, 23°13.88'W; water depth: 2311 m).

Samples for paleomagnetic analysis were taken approximately every 25 cm; we avoided sediment section that showed any sign of disturbance. Only orientation with respect to the vertical axis was preserved so that the inclination component was used to infer polarity at this high-latitude site. Natural remanent magnetization (NRM) was measured on a two-axis cryogenic magnetometer (Goree and Fuller, 1976) both before and after alternating-field demagnetization at 10 to 30 mT. NRM intensities are typically of the order 10^{-2} A/m in the upper 45 m of the section, decreasing to about 10^{-3} A/m in the lower part. Inclinations are generally well grouped near to the expected dipole valve (71 degrees, positive for normal and negative for reversed) for the latitude of the site. A reliable record of the geomagnetic field was obtained to the base of the Gauss normal magnetochron (Fig. 6). The lower boundary of the Olduvai subchron is obscured by disturbance at the break between successive cores, while the Mammoth subchron is unclear, probably lying in a slightly disturbed section at the top of Core 11.

Stable oxygen and carbon isotope analyses were made at intervals of approximately 10 cm from well below the first ice-rafting layer through to the recent sediment (Figs. 7–9). The sample was dispersed by shaking for a few hours in distilled water, and sieved on a 150 μm screen. The portion retained was dried at 60°C and weighed; the fine fraction was settled for 24 hr., dried, and weighed; the residue was retained for nannofossil studies (Backman, this volume). Three species were utilized for stable isotope analysis: *Globocassidulina subglobosa, Uvigerina peregrina*, and *Planulina wuellerstorfi*. Standard techniques for analysis were used: reaction with 100% orthophosphoric acid at 50°C, removal of water, and isotopic analysis in a VG Isogas 903 triple collector mass spectrometer. Overall analytical uncertainty during the time these measurements were made was ±0.07‰ (0–18) and ±0.05‰ (C-13) (both 1-sigma valves). A more complete description of these techniques and tables of analytical results and calibrations are given in Shackleton et al. (1984) and Shackleton and Hall (this volume).

LITHOLOGIC DESCRIPTION

Hole 552A is located at a water depth of 2311 m on the Hatton Sediment Drift at the base of the western flank of Rockall Plateau (Site 552 chapter, Figs. 1, 2). The drift sediments are thought to have been deposited under bottom currents flowing northeastward unparallel to the slope. According to McCave et al. (1980), this flow consists of Iceland–Scotland Overflow Water which has rounded the southern end of the plateau after having passed over Feni Drift in the Rockall Trough.

The uppermost sediments are Plio–Pleistocene in age and are characterized by alternating beds of foraminiferal–nannofossil ooze and calcareous marls and mud. These extend from the seafloor to a basal contact defined by the lowermost marl in this unit (Section 552A-9-4; 43.6 m sub-bottom), which is also defined by the base of high magnetic intensity. This part of the section was continuously cored with the HPC; with the exception of Core 6 (24–29 m sub-bottom), most of the cores were undisturbed, as indicated by the well-defined stratigraphic contacts and sedimentological details.

One of the most striking characteristics of this unit is the cyclicity of color and carbonate content (Fig. 7A, B). Color cycles are clearly coupled with carbonate content, the lighter shades correlating with high carbonate values. In this part of the North Atlantic, variation in

Table 1. Calcium carbonate data, Hole 552A.

Depth (m)	Core-Section (level in cm)	$CaCO_3$ (%)	CF (%)	CF $CaCO_3$ (%)
0.08	1-1, 7	80	44	85
0.16	1-1, 15	82	62	90
0.21	1-1, 20	76	51	84
0.31	1-1, 30	52	41	66
0.39	1-1, 38	34	23	69
0.49	1-1, 48	34		
0.61	1-1, 60	28	27	56
0.69	1-1, 68	20	16	62
0.80	1-1, 79	33	18	77
0.91	1-1, 90	37	29	64
1.00	1-1, 99	33	19	79
1.10	1-1, 109	46	34	74
1.19	1-1, 118	39	27	69
1.29	1-1, 128	51		
1.42	1-1, 141	41	23	77
1.52	1-2, 1	21	17	17
1.61	1-2, 10	55	35	82
1.71	1-2, 20	70	30	86
1.79	1-2, 28	67	38	78
1.90	1-2, 39	82	43	87
2.01	1-2, 50	77		
2.15	1-2, 64	81	46	92
2.19	1-2, 68	83		
2.30	1-2, 79	61	25	79
2.41	1-2, 90	25	27	85
2.49	1-2, 98	28	18	53
2.60	1-2, 109	42	18	91
2.71	1-2, 120	35	15	6
2.80	1-2, 129	23	14	68
2.95	1-2, 144	45	32	71
3.02	1-3, 1	64	45	82
3.10	1-3, 9	42	42	71
3.20	1-3, 19	50	41	77
3.31	1-3, 30	62	50	81
3.45	1-3, 44	70		
3.50	1-3, 49	68	34	84
3.59	1-3, 58	63	38	80
3.70	1-3, 69	41	25	80
3.79	1-3, 78	65	37	86
3.89	1-3, 88	72	39	92
3.99	1,CC (4)	50	25	69
4.05	1,CC (10)	50	21	65
4.29	2-1, 28	34	22	66
4.41	2-1, 40	44	25	76
4.50	2-1, 49	29	17	57
4.60	2-1, 59	33	24	65
4.70	2-1, 69	44	22	71
4.81	2-1, 80	77	32	86
4.91	2-1, 90	71	38	86
4.99	2-1, 98	60		
5.11	2-1, 110	75	34	87
5.20	2-1, 119	68	31	88
5.31	2-1, 130	71	33	89
5.40	2-1, 139	66	37	85
5.52	2-2, 1	84	44	93
5.61	2-2, 10	81		
5.72	2-2, 21	44	23	74
5.76	2-2, 25	52	28	69
5.81	2-2, 30	53	54	60
5.90	2-2, 39	72	24	92
6.00	2-2, 49	78	26	86
6.10	2-2, 59	72	36	93
6.15	2-2, 64	79	35	96
6.21	2-2, 70	88	12	98
6.26	2-2, 75	91	16	100
6.32	2-2, 81	91	16	98
6.41	2-2, 90	91	19	97
6.50	2-2, 99	87		
6.61	2-2, 110	87	15	90

Table 1. (Continued).

Depth (m)	Core-Section (level in cm)	$CaCO_3$ (%)	CF (%)	CF $CaCO_3$ (%)
6.71	2-2, 120	83	21	88
6.81	2-2, 130	46	15	80
6.91	2-2, 140	46	13	
7.02	2-3, 1	32	22	33
7.11	2-3, 10	15	21	
7.20	2-3, 19	12	12	29
7.31	2-3, 30	23	29	48
7.39	2-3, 38	34		
7.51	2-3, 50	29	15	60
7.61	2-3, 60	34	24	57
7.69	2-3, 68	42	19	71
7.79	2-3, 78	78	22	48
7.92	2-3, 91	44	28	69
8.01	2-3, 100	42	20	69
8.09	2-3, 108	44	19	72
8.21	2-3, 120	44	22	65
8.30	2-3, 129	45	16	60
8.40	2-3, 139	33	10	64
8.52	2-4, 1	67	19	87
8.55	2-4, 4	88	16	83
8.61	2-4, 10	76	10	80
8.68	2-4, 17	49	5	65
8.75	2-4, 24	81		
8.81	2-4, 30	88	14	81
8.89	2-4, 38	88	16	91
8.98	2,CC (8)	90	36	95
9.02	3-1, 1	69	22	85
9.11	3-1, 10	49	14	73
9.21	3-1, 20	66	20	75
9.31	3-1, 30	66	21	85
9.41	3-1, 40	27	11	67
9.48	3-1, 47	76	13	76
9.58	3-1, 57	82	13	78
9.69	3-1, 68	64	24	76
9.79	3-1, 78	42	27	74
9.87	3-1, 86	77	46	92
9.98	3-1, 97	79	35	86
10.06	3-1, 105	71	28	80
10.18	3-1, 117	79	50	87
10.30	3-1, 129	80	54	88
10.37	3-1, 136	85		
10.55	3-2, 4	79	43	87
10.68	3-2, 17	64	41	76
10.75	3-2, 24	31	17	56
10.84	3-2, 33	25	21	41
10.88	3-2, 37	25	14	66
10.98	3-2, 47	49	35	85
11.14	3-2, 63	14	24	59
11.24	3-2, 73	23	21	47
11.34	3-2, 83	34	23	67
11.39	3-2, 88	24		
11.44	3-2, 93	22	23	50
11.50	3-2, 99	15	12	67
11.64	3-2, 113	26	13	60
11.73	3-2, 122	40	21	72
11.84	3-2, 133	23	10	56
11.97	3-2, 146	33	16	67
12.04	3-3, 3	28	24	73
12.13	3-3, 12	31	19	57
12.20	3-3, 19	3(ash)	15	10
12.33	3-3, 32	45	21	60
12.45	3-3, 44	29	15	76
12.50	3-3, 49	83	54	96
12.58	3-3, 57	89	37	92
12.64	3-3, 63	84	36	95
12.75	3-3, 74	77	34	91
12.85	3-3, 84	66	29	77
12.94	3-3, 93	43	16	70
12.98	3-3, 97	42		

Table 1. (Continued).

Depth (m)	Core-Section (level in cm)	$CaCO_3$ (%)	CF (%)	CF $CaCO_3$ (%)
13.15	3-3, 114	4	6	17
13.19	3-3, 118	8		
13.22	3-3, 121	10	9	23
13.30	3-3, 129	17	15	67
13.40	3-3, 139	40	28	87
13.47	3-3, 146	57		
13.54	3-4, 3	71	46	91
13.63	3-4, 12	62	35	82
13.75	3-4, 24	49	27	90
13.78	3-4, 27	18	19	55
13.95	3,CC (15)	18	16	50
14.02	4-1, 1	48	24	80
14.11	4-1, 10	52	31	82
14.21	4-1, 20	70	16	60
14.31	4-1, 30	59	22	74
14.42	4-1, 41	18	21	27
14.52	4-1, 51	14	6	38
14.60	4-1, 59	73	27	53
14.72	4-1, 71	61	32	65
14.80	4-1, 79	64	43	83
14.90	4-1, 89	79	41	86
15.12	4-1, 111	80	33	88
15.20	4-1, 119	67	35	83
15.30	4-1, 129	76		
15.40	4-1, 139	75	43	85
15.52	4-2, 1	78	41	86
15.62	4-2, 11	77	27	
15.70	4-2, 19	41	24	49
15.79	4-2, 28	37	28	49
15.92	4-2, 41	33		
16.01	4-2, 50	21	16	48
16.10	4-2, 59	8	18	34
16.19	4-2, 68	7	13	12
16.30	4-2, 79	9	3	8
16.41	4-2, 90	10	4	50(?)
16.51	4-2, 100	19		
16.62	4-2, 111	60	39	85
16.71	4-2, 120	60	40	86
16.78	4-2, 127	60	33	80
16.89	4-2, 138	36	11	59
16.96	4-2, 145	16	5	23
17.02	4-3, 1	18	19	44
17.10	4-3, 9	4	24	37
17.20	4-3, 19	50	25	75
17.30	4-3, 29	49		
17.39	4-3, 38	64	50	68
17.49	4-3, 48	88	40	89
17.60	4-3, 59	55	28	82
17.71	4-3, 70	10	20	17
17.81	4-3, 80	70	39	89
17.86	4-3, 85	79	50	84
17.91	4-3, 90	62	31	79
18.02	4-3, 101	47		
18.06	4-3, 105	49	25	80
18.13	4-3, 112	18	10	45
18.20	4-3, 119	3	6	33(?)
18.31	4-3, 130	60	41	86
18.42	4-3, 141	69	38	88
18.52	4-4, 1	52	35	87
18.61	4-4, 10	28	10	56
18.68	4-4, 17	11	7	38
18.71	4-4, 20	34	18	77
18.81	4-4, 30	53	31	84
18.89	4,CC (8)	51	22	80
18.98	4,CC (17)	28	19	72
19.02	5-1, 1	63	40	87
19.09	5-1, 8	37	16	71
19.20	5-1, 19	56	33	77
19.31	5-1, 30	74	61	82

Table 1. (Continued).

Depth (m)	Core-Section (level in cm)	$CaCO_3$ (%)	CF (%)	CF $CaCO_3$ (%)
19.40	5-1, 39	72	43	85
19.56	5-1, 55	56	35	71
19.61	5-1, 60	36	18	56
19.72	5-1, 71	33	25	77
19.80	5-1, 79	62	29	78
19.91	5-1, 90	91	38	96
19.97	5-1, 96	89	36	93
20.12	5-1, 111	83	44	91
20.20	5-1, 119	75	41	88
20.30	5-1, 129	59	35	89
20.43	5-1, 142	16	24	71
20.52	5-2, 1	31	24	75
20.59	5-2, 8	26	8	35
20.70	5-2, 19	68	31	77
20.81	5-2, 30	10	9	54
20.92	5-2, 41	9	43	86
21.03	5-2, 52	34	5	58
21.11	5-2, 60	43	46	58
21.23	5-2, 72	23	18	62
21.32	5-2, 81	41	16	65
21.41	5-2, 90	69	44	79
21.49	5-2, 98	86	51	92
21.58	5-2, 107	85	49	87
21.71	5-2, 120	70	57	89
21.82	5-2, 131	31	24	64
21.93	5-2, 142	35		
22.02	5-3, 1	45	40	42
22.10	5-3, 9	39	13	73
22.20	5-3, 19	41	17	77
22.32	5-3, 31	64	53	74
22.43	5-3, 42	84	28	90
22.53	5-3, 52	63	15	60
22.61	5-3, 60	47	37	79
22.69	5-3, 68	16	10	37
22.81	5-3, 80	37	17	56
22.91	5-3, 90	48	30	63
23.01	5-3, 100	54	31	78
23.11	5-3, 110	77	42	86
23.20	5-3, 119	49	31	39
23.31	5-3, 130	17	15	33
23.43	5-3, 142	45	11	78
23.52	5-4, 1	29	14	24
23.63	5-4, 12	4	5	0
22.67	5-4, 16	12		
23.71	5-4, 20	19	6	9
23.81	5-4, 30	72	42	80
23.91	5-4, 40	85	41	89
23.95	5,CC (4)	84	39	92
24.03	5,CC (12)	36	17	25
29.08	7-1, 7	54	36	57
29.19	7-1, 18	56		
29.29	7-1, 28	82	51	85
29.39	7-1, 38	72	37	89
29.49	7-1, 48	78	44	94
29.61	7-1, 60	89	39	95
29.72	7-1, 71	84	30	96
29.82	7-1, 81	79	36	87
29.90	7-1, 89	52	39	75
29.99	7-1, 98	53	30	85
30.09	7-1, 108	83	39	93
30.21	7-1, 120	83	54	92
30.32	7-1, 131	72	43	77
30.42	7-1, 141	54	28	62
30.52	7-2, 1	15	33	0
30.61	7-2, 10	30	17	47
30.72	7-2, 21	28	13	57
30.81	7-2, 30	15	13	2
30.92	7-2, 41	59	28	84
31.01	7-2, 50	17	12	35

Table 1. (Continued).

Depth (m)	Core-Section (level in cm)	$CaCO_3$ (%)	CF (%)	CF $CaCO_3$ (%)
31.10	7-2, 59	54	30	86
31.19	7-2, 68	84	29	90
31.28	7-2, 77	84	44	88
31.39	7-2, 88	46	40	69
31.54	7-2, 103	33	21	74
31.59	7-2, 108	7	12	47
31.70	7-2, 119	85	49	97
31.82	7-2, 131	87	40	96
31.88	7-2, 137	89		
31.96	7-2, 145	85	37	92
32.02	7-3, 1	84	46	91
32.12	7-3, 11	66	25	83
32.22	7-3, 21	52	17	50
32.31	7-3, 30	13	9	0
32.38	7-3, 37	46	17	
32.54	7-3, 53	40	14	72
32.59	7-3, 58	81	37	86
32.68	7-3, 67	77	32	85
32.83	7-3, 82	77	29	87
32.87	7-3, 86	58	16	76
32.99	7-3, 98	24	9	41
33.12	7-3, 111	85	39	92
33.20	7-3, 119	89	44	96
33.32	7-3, 131	90	50	96
33.46	7-3, 145	89		
33.52	7-4, 1	89	40	98
33.57	7-4, 6	88	29	95
33.67	7,CC (6)	89	37	96
33.77	7,CC (16)	88	39	95
34.03	8-1, 2	60	33	69
34.09	8-1, 8	18	4	7
34.19	8-1, 18	68	32	75
34.31	8-1, 30	66	25	80
34.43	8-1, 42	66	22	84
34.50	8-1, 49	71	29	
34.58	8-1, 57	72	36	78
34.69	8-1, 68	83	39	86
34.79	8-1, 78	80	39	89
34.88	8-1, 87	81	39	90
34.99	8-1, 98	61		
35.11	8-1, 111	73	24	85
35.20	8-1, 119	63	24	81
35.32	8-1, 131	71	25	86
35.46	8-1, 145	55	23	89
35.52	8-2, 1	79	38	98
35.61	8-2, 10	88	33	96
35.68	8-2, 17	92		
35.81	8-2, 30	90	37	98
35.92	8-2, 41	88	33	98
36.01	8-2, 50	89	28	98
36.11	8-2, 60	90	36	100
36.21	8-2, 70	87	29	96
36.31	8-2, 80	87	27	97
36.41	8-2, 90	87	31	97
36.52	8-2, 101	86	21	94
36.61	8-2, 110	87	26	97
36.66	8-2, 115	89	34	96
36.81	8-2, 130	84	14	94
36.96	8-2, 145	53	14	77
37.02	8-3, 1	55	31	63
37.09	8-3, 8	53	14	67
37.18	8-3, 17	29		
37.31	8-3, 30	61	26	76
37.41	8-3, 40	58	15	72
37.53	8-3, 52	72		
37.61	8-3, 60	79	26	84
37.72	8-3, 71	49	12	72
37.79	8-3, 78	68	16	87
37.87	8-3, 86	86	33	89

Table 1. (Continued).

Depth (m)	Core-Section (level in cm)	$CaCO_3$ (%)	CF (%)	CF $CaCO_3$ (%)
37.95	8-3, 94	79	13	90
38.01	8-3, 100	68	20	78
38.13	8-3, 112	38	14	49
38.21	8-3, 120	6	31	4
38.29	8-3, 128	29	11	50
38.42	8-3, 141	74	42	93
38.52	8-4, 1	90	36	?
38.61	8-4, 10	79	33	90
38.71	8-4, 20	85	34	93
38.81	8-4, 30	78	47	89
38.90	8-4, 39	83	34	91
38.97	8,CC (6)	31	12	54
39.06	9-1, 5	77	37	88
39.16	9-1, 15	73	31	88
39.34	9-1, 33	85	26	92
39.48	9-1, 47	81	19	94
39.65	9-1, 64	46	20	47
39.75	9-1, 74	33	26	86
39.95	9-1, 94	84	46	85
40.00	9-1, 99	78		
40.07	9-1, 106	58	30	77
40.17	9-1, 116	87	41	92
40.28	9-1, 127	80	29	89
40.40	9-1, 139	56	22	71
40.48	9-1, 147	86	35	100
40.56	9-2, 5	85	45	92
40.66	9-2, 15	81	36	87
40.78	9-2, 27	68	32	71
40.90	9-2, 39	35	20	46
40.96	9-2, 45	29	35	40
41.07	9-2, 56	80	40	83
41.18	9-2, 67	84	37	85
41.28	9-2, 77	64	21	70
41.35	9-2, 84	24	14	40
41.38	9-2, 87	62	44	60
41.47	9-2, 96	82		
41.55	9-2, 104	81	17	92
41.61	9-2, 110	82	22	90
41.69	9-2, 118	55	23	62
41.79	9-2, 128	15	6	58
41.86	9-2, 135	52	22	58
41.98	9-2, 147	23		
41.99	9-2, 148	21	22	30
42.06	9-3, 5	27	19	24
42.14	9-3, 13	44	26	73
42.18	9-3, 17	92		
42.28	9-3, 27	90	25	97
42.39	9-3, 38	92	28	100
42.49	9-3, 48	92	36	100
42.58	9-3, 57	90	34	98
42.69	9-3, 68	90	34	100
42.79	9-3, 78	93	24	98
42.95	9-3, 94	90	20	97
43.07	9-3, 106	90	26	100
43.16	9-3, 115	90	27	91
43.18	9-3, 117	67	27	94
43.28	9-3, 127	88	19	98
43.40	9-3, 139	78	14	85
43.50	9-3, 149	60	20	64
43.56	9-4, 5	78	50	92
43.66	9-4, 15	89	26	93
43.77	9-4, 26	87	37	88
43.92	9,CC (13)	86	31	92
44.02	10-1, 1	83	35	90
44.12	10-1, 11	85	24	68
44.26	10-1, 25	93	23	97
44.32	10-1, 31	91	32	93
44.43	10-1, 42	92	30	97
44.53	10-1, 52	89	17	100

Table 1. (Continued).

Depth (m)	Core-Section (level in cm)	$CaCO_3$ (%)	CF (%)	CF $CaCO_3$ (%)
44.61	10-1, 60	90	11	
44.73	10-1, 72	92	16	100
44.83	10-1, 82	94	22	97
44.88	10-1, 87	92		
44.93	10-1, 92	89	21	98
45.04	10-1, 103	91	19	100
45.08	10-1, 107	92		
45.23	10-1, 122	91	28	96
45.30	10-1, 129	92	25	97
45.49	10-1, 148	92	21	98
45.54	10-2, 3	89	34	93
45.63	10-2, 12	90	34	95
45.72	10-2, 21	91	46	91
45.82	10-2, 31	83	36	93
45.96	10-2, 45	87	45	92
46.03	10-2, 52	90	25	96
46.13	10-2, 62	91	34	95
46.23	10-2, 72	92	39	94
46.34	10-2, 83	92	32	96
46.42	10-2, 91	89	22	97
46.53	10-2, 102	89	24	100
46.58	10-2, 107	90		
46.64	10-2, 113	92	27	98
46.72	10-2, 121	93	32	96
46.80	10-2, 129	91	24	98
46.88	10-2, 137	92		
46.96	10-2, 145	92	28	100
47.04	10-3, 3	89	26	99
47.12	10-3, 11	92	19	98
47.22	10-3, 21	91	15	100
47.31	10-3, 30	88	18	97
47.43	10-3, 42	92	15	100
47.55	10-3, 54	93	18	100
47.63	10-3, 62	93	27	99
47.73	10-3, 72	92	23	100
47.85	10-3, 84	94	22	100
47.93	10-3, 92	92	30	99
48.06	10-3, 105	93	23	100
48.13	10-3, 112	92	26	98
48.23	10-3, 122	93	40	98
43.25	10-3, 134	92	30	98
48.47	10-3, 146	92		
48.54	10-4, 3	92	31	98
48.67	10-4, 16	93	19	85
48.76	10-4, 25	90	19	100
48.78	10-4, 27	87	23	95
48.90	10-4, 39	94	19	98
49.01	10,CC (8)	90	18	100
49.07	11-1, 6	83	27	79
49.21	11-1, 20	90	19	98
49.29	11-1, 28	92	25	100
49.41	11-1, 40	90	15	100
49.51	11-1, 50	89	22	98
49.59	11-1, 58	91	25	98
49.71	11-1, 70	84	21	84
49.80	11-1, 79	89	19	100
49.88	11-1, 87	92	20	98
50.00	11-1, 99	92	16	100
50.11	11-1, 110	93	16	100
50.18	11-1, 117	93	22	100
50.31	11-1, 130	93	18	97
50.41	11-1, 140	92	21	93
50.55	11-2, 4	93	26	97
50.64	11-2, 13	91	14	97
50.70	11-2, 19	91	15	94
50.85	11-2, 34	91	18	88
50.91	11-2, 40	92	14	97
50.98	11-2, 47	91		
51.09	11-2, 58	89	25	99
51.24	11-2, 73	90	12	93

Table 1. (Continued).

Depth (m)	Core-Section (level in cm)	$CaCO_3$ (%)	CF (%)	CF $CaCO_3$ (%)
51.43	11-2, 92	92	15	95
51.53	11-2, 102	93	10	96
51.66	11-2, 115	94	7	95
51.68	11-2, 117	93	9	96
51.79	11-2, 128	91	11	96
51.89	11-2, 138	92	16	96
52.05	11-3, 4	91	17	94
52.14	11-3, 13	91	15	97
52.24	11-3, 23	92	15	100
52.33	11-3, 32	92	26	99
52.38	11-3, 37	93		
52.48	11-3, 47	93		
52.58	11-3, 57	94	26	94
52.75	11-3, 74	95	15	100
52.87	11-3, 86	94	17	96
52.98	11-3, 97	93		
53.09	11-3, 108	95	10	96
53.23	11-3, 122	93	9	97
53.35	11-3, 134	92	6	93
53.55	11-4, 4	92	8	96
53.67	11-4, 16	93	8	100
53.78	11-4, 27	92	11	97
53.90	11-4, 39	95	7	88
54.02	11,CC (8)	94	11	94
54.07	12-1, 6	88	17	76
54.20	12-1, 19	93	14	84
54.33	12-1, 32	95	13	95
54.40	12-1, 39	92	7	88
54.55	12-1, 54	93	7	91
54.63	12-1, 62	92	10	93
54.75	12-1, 74	94	6	100
54.85	12-1, 84	94	9	96
54.91	12-1, 90	94	12	96
55.08	12-1, 107	94	13	100
55.23	12-1, 122	91	13	98
55.36	12-1, 135	90	11	100
55.49	12-1, 148	91	12	100
55.55	12-2, 4	93	15	98
55.66	12-2, 15	92	13	100
55.75	12-2, 24	93	12	100
55.83	12-2, 32	93	21	95
55.95	12-2, 44	93	11	100
56.08	12-2, 57	92	19	95
56.19	12-2, 68	93	18	98
56.29	12-2, 78	94	17	100
56.41	12-2, 90	93	18	97
56.53	12-2, 102	92	16	97
56.68	12-2, 117	91	24	95
56.79	12-2, 128	91	9	100
56.95	12-2, 144	90	8	100
57.04	12-3, 3,	87	11	88
57.08	12-3, 8	88		
57.17	12-3, 16	89	11	100
57.33	12-3, 32	94	11	95
57.46	12-3, 45	93	10	97
57.59	12-3, 58	94	13	96
57.75	12-3, 74	93	14	100
57.78	12-3, 77	94		
57.91	12-3, 90	90	9	93
57.98	12-3, 97	91	7	100
58.16	12-3, 115	89	9	100
58.19	12-3, 118	87	9	100
58.30	12-3, 129	92	9	100
58.39	12-3, 138	91	9	100
58.54	12-4, 3	95	9	100
58.66	12-4, 15	87		
58.74	12-4, 23	93	7	100
58.78	12-4, 27	95	9	100
58.86	12,CC (5)	91	11	100
58.96	12,CC (15)	92	10	96

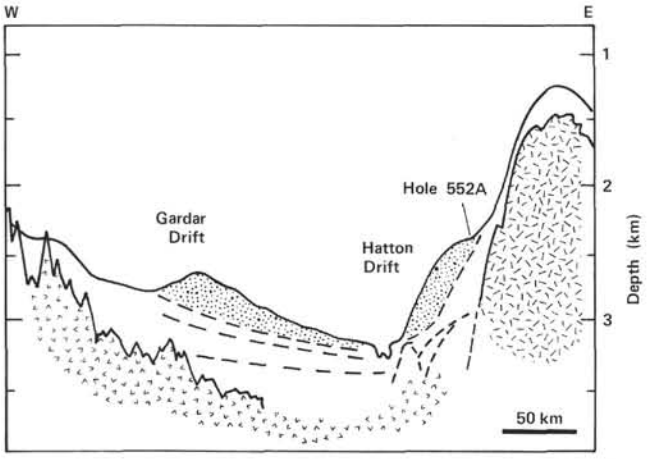

Figure 2. Position of Hole 552A on the western flank of Rockall Plateau. Sediments of the Gardar and Hatton drifts are stippled. Subbottom information generalized from Site 552 chapter (this volume).

the carbonate content is controlled by glacial–interglacial depositional regimes (Ruddiman and McIntyre, 1976); coccoliths and foraminifers are deposited two to three times more rapidly during interglacials (a function of surface water productivity), whereas noncalcareous terrigenous sediments are deposited more rapidly under glacial climatic conditions as a result of ice-rafting.

Biogenous Constituents

The calcareous oozes occur in shades of white and light gray and are somewhat mottled by bioturbation. Laminated structures are rare, although an occasional thin layer (<1 cm thick) of foraminiferal "sand" may result from winnowing by bottom currents. The carbonate content of the interglacial calcareous oozes fluctuates between 70 and 90%, attaining a consistent value of 95% in the underlying late Pliocene preglacial oozes below 44 m (Fig. 3).

Carbonate content is clearly correlated with the coarse fraction (>74 μm) content. Even a cursory examination of the sediment reveals that the largest proportion of the coarse fraction of the interglacial stages consists of foraminiferal tests (Fig. 3). Except for the low-carbonate spikes during glacial episodes, most of the coarse fraction is of high carbonate content. It is interesting to note that during interglacial stages the coarse fraction components (foraminifers) form 40 to 60% of the total sediment, whereas in the preglacial late Pliocene oozes, the coarse fraction makes up generally less than 20% of the sediment.

The interplay between these three curves—carbonate percent, coarse fraction percent, and carbonate percent of the coarse fraction (Fig. 3)—reflects the variation of the calcareous components produced under the rapidly changing climatic regimes of the past 2.4 m.y. The low carbonate–low productivity segments of the carbonate curve most probably reflect the prevalence of sea ice and downwelling within the broadly cyclonic circulation of surface water in the Rockall–Greenland sector of the glacial North Atlantic. Under interglacial conditions the return of the warm North Atlantic Drift stimulates an increase in biologic productivity. The spikes of low coarse fraction carbonate associated with the glacial stages suggest particularly intense cold periods during which sea-ice cover may have been so extensive that surface productivity in this area was effectively eliminated for periods of time long enough to be recorded in this section.

There is also a positive correlation between biogenic silica and total carbonate content (Baldauf, this volume). Biosiliceous productivity thus corresponds to that of the calcareous microfossils. Biogenic silica, however, only becomes abundant where carbonate content exceeds 90%. Sponge spicules occur commonly in sediments with carbonate values as low as 80%; the more delicate diatoms and radiolarians, however, only occur in sediments of higher carbonate content. The correspondence of diatom and calcareous microfossil abundance suggests that planktonic productivity of both is controlled by similar climatically induced environmental factors in the surface ocean.

A particularly distinct interval of biosiliceous dissolution, occurring between 8 and 33 m sub-bottom (0.44–1.8 m.y., Fig. 9; Baldauf, this volume), does not allow a complete correlation of siliceous/calcareous planktonic productivity. Although occasional samples within this interval contain well-preserved diatom flora, the majority of samples are barren of diatoms. This barren interval has probably resulted from a complex of environmental factors affecting productivity and preservation. An interval which may be similar was recorded by Schrader and Fenner (1976) in the Norwegian Sea (DSDP Leg 38). At these sites, the barren interval was also punctuated by occasional samples with an abundant assemblage of temperate diatoms. It is suggested that these occurrences of abundant diatom content represent isolated episodes of warmth during which the North Atlantic Drift is able to penetrate into the Norwegian Sea.

Organic carbon content (Kaltenback et al., this volume) also has a cyclical variability. Interglacial carbonate oozes have organic carbon contents of 0.06–0.08%, whereas in the glacial muds the organic carbon values are in the 0.14–0.20% range (Fig. 4). Analysis by Rock-Eval pyrolysis also reveals that organic carbon content of glacial sediments contains a higher proportion of residual or reworked carbon (commonly termed "highly oxidized, residual nonsource," Fig. 5). The higher levels of organic carbon, therefore, reflect an influx of reworked organic matter during glacial climates, undoubtedly a result of lower sea levels and increased erosion of the continents and continental shelves.

Sediments enriched in organic phosphorus often characterize organic material of pelagic origin. Interglacial organic material of these sediments is enriched in phosphorus (c/p < 25), whereas in glacial sediments organic phosphorus was not detected. Relatively high levels of organic phosphorus also characterize the late Pliocene calcareous oozes deposited prior to the inception of glaciation. These high values of organic phosphorus considered together with the low values of residual carbon suggest a predominately marine origin for the organic material of the interglacial sediments.

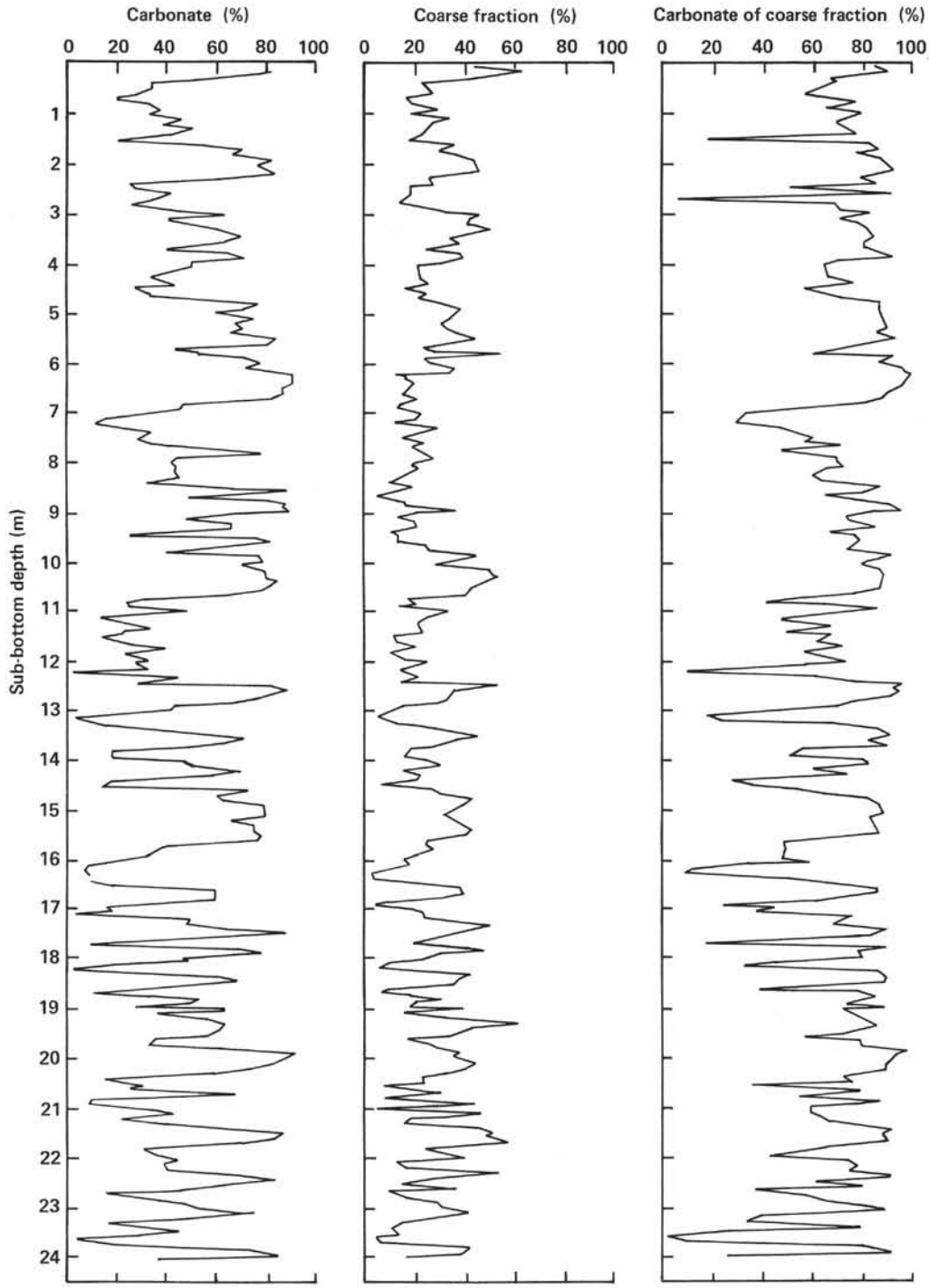

Figure 3. Percent carbonate, coarse fraction (>74 μm), and coarse fraction carbonate plotted on a depth scale, Hole 552A, Cores 1-5 and Cores 7-12.

Because of the difficulty in measuring such small amounts of organic material, samples from only two climatic cycles were examined. We note that, with respect to organic matter, there is apparently little difference between a glacial–interglacial cycle occurring early or late in the Plio–Pleistocene sequence.

Terrigenous Components

The bulk of the noncarbonate fraction of these sediments is concentrated in the glacial sequences. XRD analysis indicates that the clay composition is almost totally smectite in the interglacial oozes, whereas the glacial muds contain the predominately terrigenous clays—illite, kaolinite, and chlorite. This observation reinforces the suggestion that sediments of the glacial stages originate primarily from continental sources related to lower sea levels and increased rates of continental erosion.

The terrigenous coarse fraction is arkosic in composition (Morton, this volume); the presence of feldspar with polycrystalline and strained monocrystalline quartz and

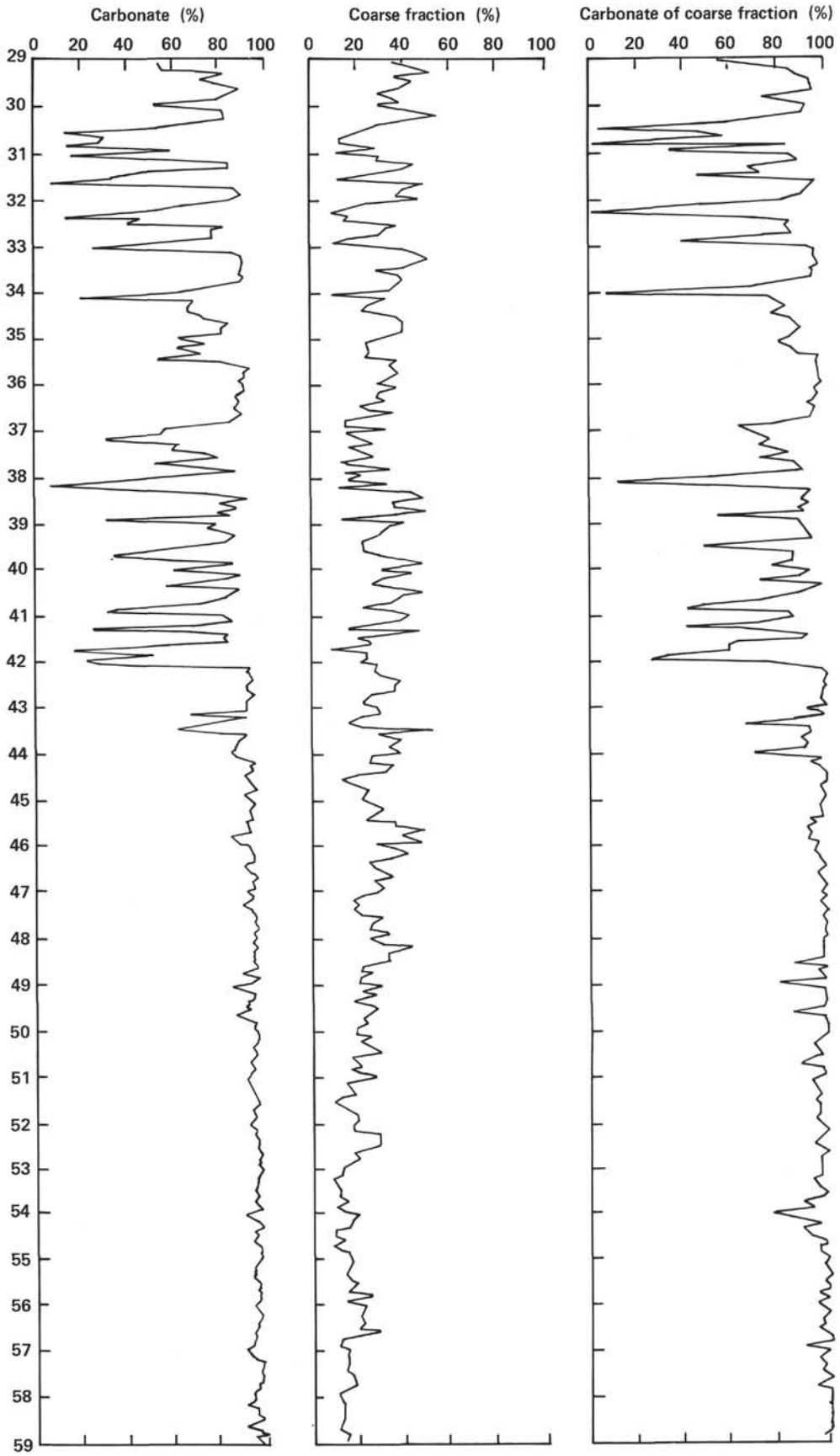

Figure 3. (Continued).

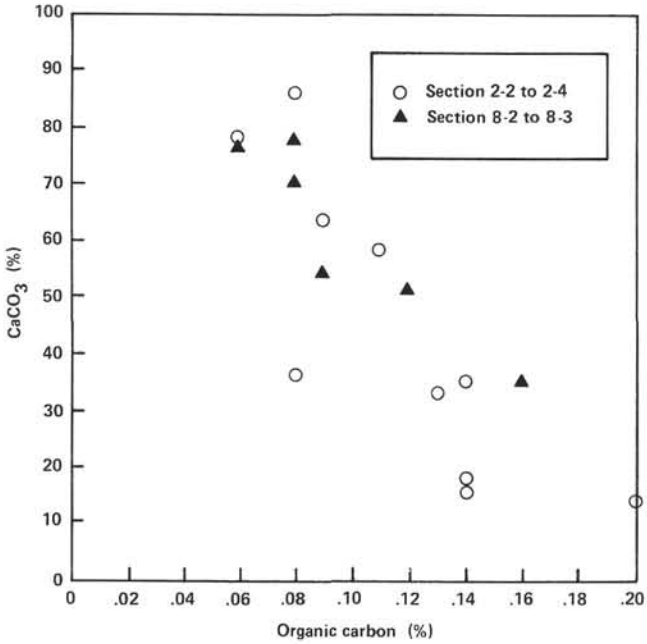

Figure 4. Percent calcium carbonate plotted against organic carbon for two climatic cycles (Hole 552A, Cores 2 and 8).

metamorphic rock fragments suggests a source largely of metamorphic basement. The occurrence of basalt grains also indicates some contribution from nearby exposed lavas. Heavy mineral constituents similarly suggest a mixed metamorphic–basaltic terrane (Morton, this volume). The most immediate single source for these sediment grains is Greenland, which satisfies the criteria of possessing both extensive tracts of metamorphic basement and large areas of exposed basalt. The sheltered position of Site 552 on the upper reaches of the Hatton Drift serves to eliminate other potential source areas to the east. Given the presence of scattered large pebbles (Site 552 chapter), ice-rafting is the most likely process of sediment transport for these sands and silts.

Pyroclastic input is sporadic; it is a consistent but relatively minor constituent in the lower part of the sequence (Cores 5 to 9), disappears in Cores 3 and 4, and is present again in Cores 1 and 2 (Morton, this volume). Most of the pyroclastic material is glassy, varying between slightly to highly vesiculated; both clear and brown types occur in variable proportions. Minor components of pyroclastic origin include augite, plagioclase, and opaque grains. These constituents of volcanic ash are similar to those of DSDP Site 404 (Harrison et al., 1979) and also to ashes of Plio–Pleistocene age at DSDP Site 346 on the Icelandic Plateau (Sylvester, 1976).

It is generally accepted that the volcanic ash of Plio–Pleistocene age in the North Atlantic and Norwegian–Greenland Sea originated from eruptions on Iceland (Ruddiman and Glover, 1972; Sylvester, 1976; Harrison et al, 1979; Donn and Ninkovitch, 1980). The explosive nature of the volcanism is ascribed to the interaction of the magma with water, in this case with glacial meltwater, in the manner described by Heiken (1975).

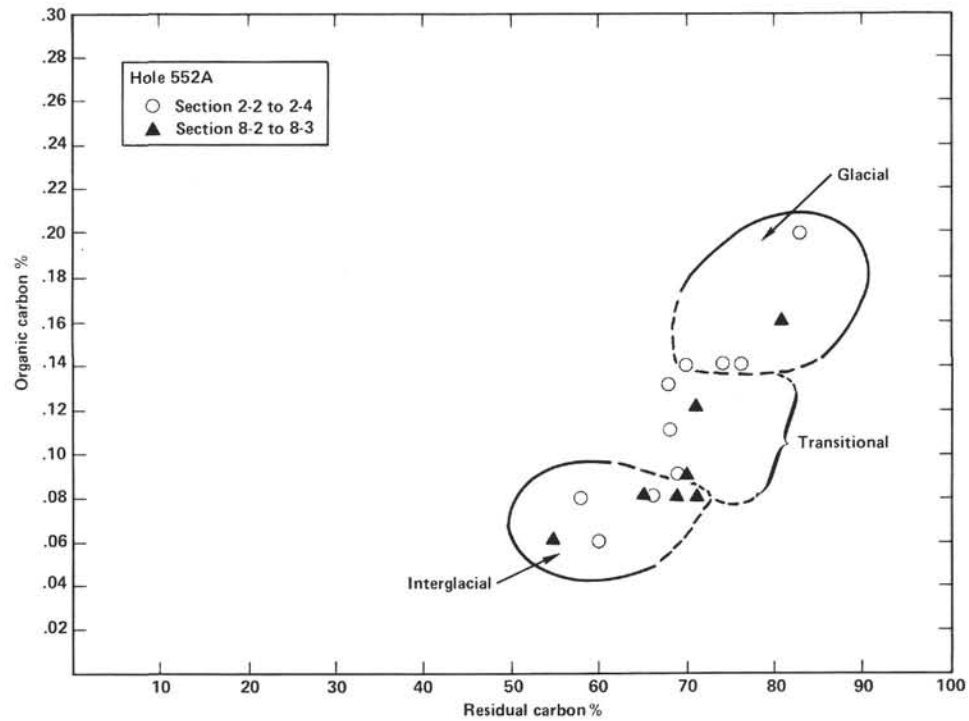

Figure 5. Percent organic carbon plotted against residual carbon for two climatic cycles (Hole 552A, Cores 2 and 8).

STABLE ISOTOPE STRATIGRAPHY

Oxygen Isotope Record: Hole 552A, Cores 1–5

In Figures 6 and 7A, the oxygen isotope, paleomagnetic, and carbonate data for the upper five cores are shown together with the oxygen isotope record of piston core V28-239 (Shackleton and Opdyke, 1976). We have used V28-239 here because, although it is known to include changes in accumulation rate, it contains an almost complete record of Plio–Pleistocene climatic cycles. A comparison of DSDP Hole 552A with V28-238, which records an almost uniform accumulation rate, may be found in Shackleton et al. (1984). Correlation of the isotopic stage boundaries reveals marked variations in accumulation rate in DSDP Hole 552A, a not unexpected result considering the lithological variations that are evident.

We have erected isotopic stage boundaries for Hole 552A by comparisons of the curves and paleomagnetic control points. For this part of the section, the global oxygen isotopic record is relatively well known. Hole 552A is clearly correlative with the Pacific record and complete to the extent of preserving every isotope stage. Shackleton and Opdyke (1973; 1976) recognized 23 isotopic stages in the late and middle Pleistocene. Through comparison of Hole 552A with the Pacific records, we have extended this numbering system to at least interglacial stage 25, which is defined as including the base of the Jaramillo subchron at 0.98 m.y. ago.

Late Pliocene Onset of Ice-rafting

The climatic record is less well known below the isotopic stages established for the middle and late Pleistocene. In Figure 8, the oxygen isotope data for the lower part of the sequence in Hole 552A is compared with the oxygen isotope data from piston core V28-179 (Shackleton and Opdyke, 1977), which covers a benthic oxygen isotope record back to 3.5 m.y. To facilitate comparison, the plotting scale for both records has been adjusted at the indicated magnetostratigraphic boundaries; an approximate age scale is thus obtained.

Comparison between these two records is good considering the low accumulation rate, bioturbation, and relatively coarse sampling interval in V28-179. The amplitude of variation, however, is substantially greater in Hole 552A than in V28-179. Since the accumulation rate of V28-179 was only about 0.55 cm/k.y., climatic extremes lasting only a few thousand years should be severely degraded by bioturbation.

Nannofossil extinction levels have been determined quantitatively for both cores and their ages estimated (Backman and Shackleton, 1983). Using these ages, the average accumulation rate over the pre–ice-rafting interval in Hole 552A is estimated at approximately 1.7 cm/k.y. This is surprisingly close to the average for the upper Pleistocene (1.8 cm/k.y.), although the rate has certainly varied over the intense climatic fluctuations represented by the alternating oozes and muds.

Paleomagnetic and nannofossil stratigraphies of the sequence in Hole 552A give identical estimates for the age of the first major northern hemisphere glacial event—2.37 m.y. Back to about 2.4 m.y. there is a remarkable correspondence between the carbonate and oxygen isotope records of Hole 552A (Fig. 7B). It is evident that both parameters are causally related to glaciation. Moreover, the coincidence of the first isotopic event with the dramatic influx of ice-rafted debris at 2.4 m.y. is clear evidence that this late Pliocene episode is related to a northern hemisphere occurrence, rather than to an Antarctic climatic event.

Comparison of the isotopic composition of benthic foraminifers at this level of the first glacial maximum with values in glacial stages in the upper part of the sequence show that the initial event represents a truly glacial interval with an ice volume similar to maxima of the middle and late Pleistocene. Although the section in Hole 552A may preserve a significant record of deep-water temperature variability in addition to the ice volume signal, the glacial event at 2.4 m.y. must certainly have been more severe than was recognized by Shackleton and Opdyke (1977). Almost a million years prior to the Pliocene/Pleistocene boundary (Backman et al., 1983), this glacial occurrence must represent the major environmental event of the late Neogene of the northern hemisphere.

Ice-rafted debris is absent prior to 2.4 m.y. This age for the initiation of major ice-rafting in the North Atlantic is considerably later than 3.0–3.2 m.y. determined by Berggren (1972) and Poore (1981). Their observations, however, were made on cores recovered by conventional

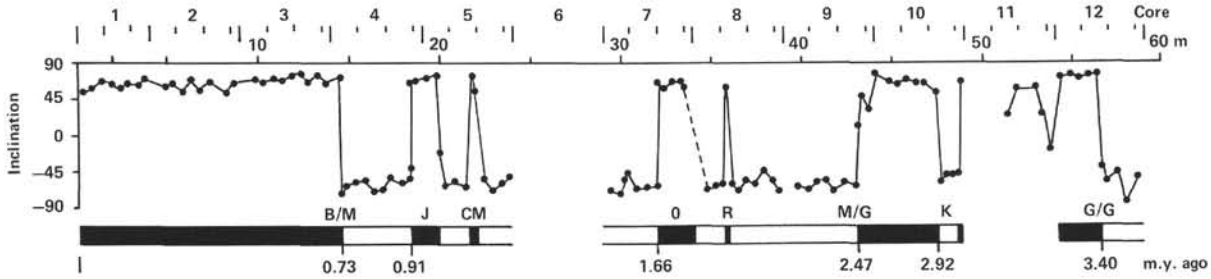

Figure 6. Magnetic record for Hole 552A, Cores 1–12. Demagnetized inclinations are shown only for apparently undisturbed parts of the cores. Time scale from Berggren et al., in press. (B = Brunhes; M = Matuyama; J = Jaramillo; CM = Cobb Mountain; O = Olduvai; R = Reunion; K = Kaena; G/G = Gauss/Gilbert.)

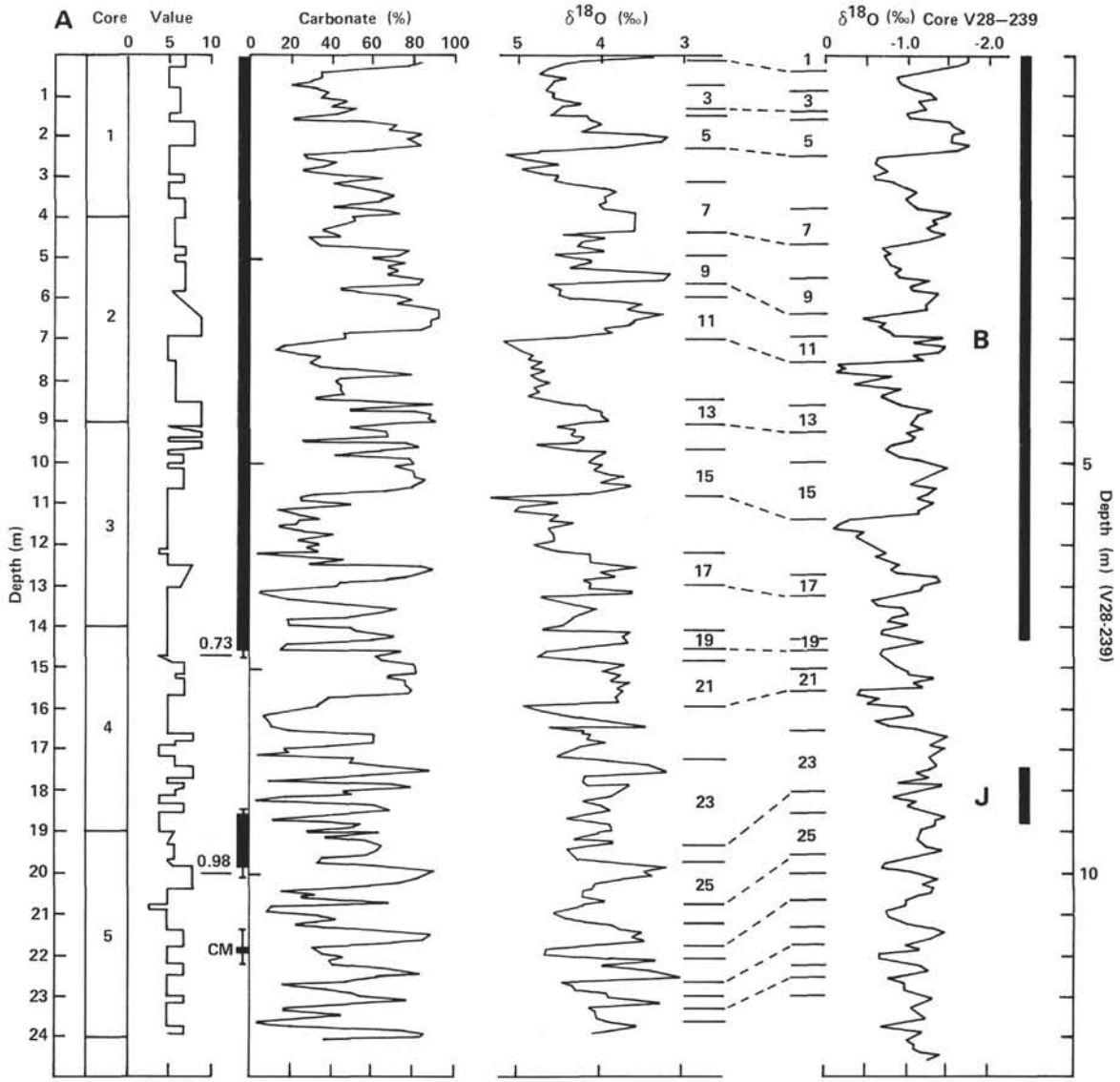

Figure 7. Summary of percent carbonate and oxygen isotope data for Hole 552A correlated with oxygen isotope record of V28-239 (Shackleton and Opdyke, 1976). Records of both cores are plotted linearly with depth. Proposed oxygen isotope stage boundaries, paleomagnetic data, and color value (light [10]–dark [1]) are also indicated. A. Cores 1-5. B. Cores 7-12.

rotary drilling in which the sediments were greatly disturbed. Backman (1979) has re-dated the inception of ice-rafted sediments at DSDP Sites 111 and 116 at 2.5 m.y. ago. Prell (1982) and Hodell et al. (1983) presented evidence of isotopic variability around 3.2 m.y. ago; Prell interpreted this as representing a brief excursion in ice volume. The record preceding the initial glacial event at Hole 552A indicates that although there was considerable climatic variability somewhere, such glaciation as may have occurred prior to 2.5 m.y. ago did not give rise to ice-rafting in the northeastern Atlantic.

Carbon Isotope Record

A water mass forming at the surface has the ^{13}C content of surface water and a high content of dissolved oxygen. During its passage through the deep reaches of the ocean, the water mass "ages"; dissolved oxygen is utilized by the oxidation of particulate organic matter sinking from the sea surface, and dissolved CO_2 becomes isotopically lighter as a consequence of the addition of this isotopically light carbon (Kroopnick, 1980; Shackleton and Hall, this volume).

Carbon isotope records of Hole 552A and piston core V28-179 are compared in Figure 9. The data are plotted on the same isotopic scale, and the same species-dependent correction factors have been applied (Shackleton et al., 1984). In today's ocean there is an observed difference of a little over 1‰ between the two areas, reflecting the fact that the deep ocean is ventilated (younger water mass) in the North Atlantic. It is clear from the persistent offset in values that the water mass bathing Hatton Drift was younger than that of the deep Pacific throughout the interval studied. Moreover, since the high-frequency variability was approximately the same prior to the major climatic event at 2.4 m.y. ago as after, the ^{13}C variability was not forced by climatic cyclicity.

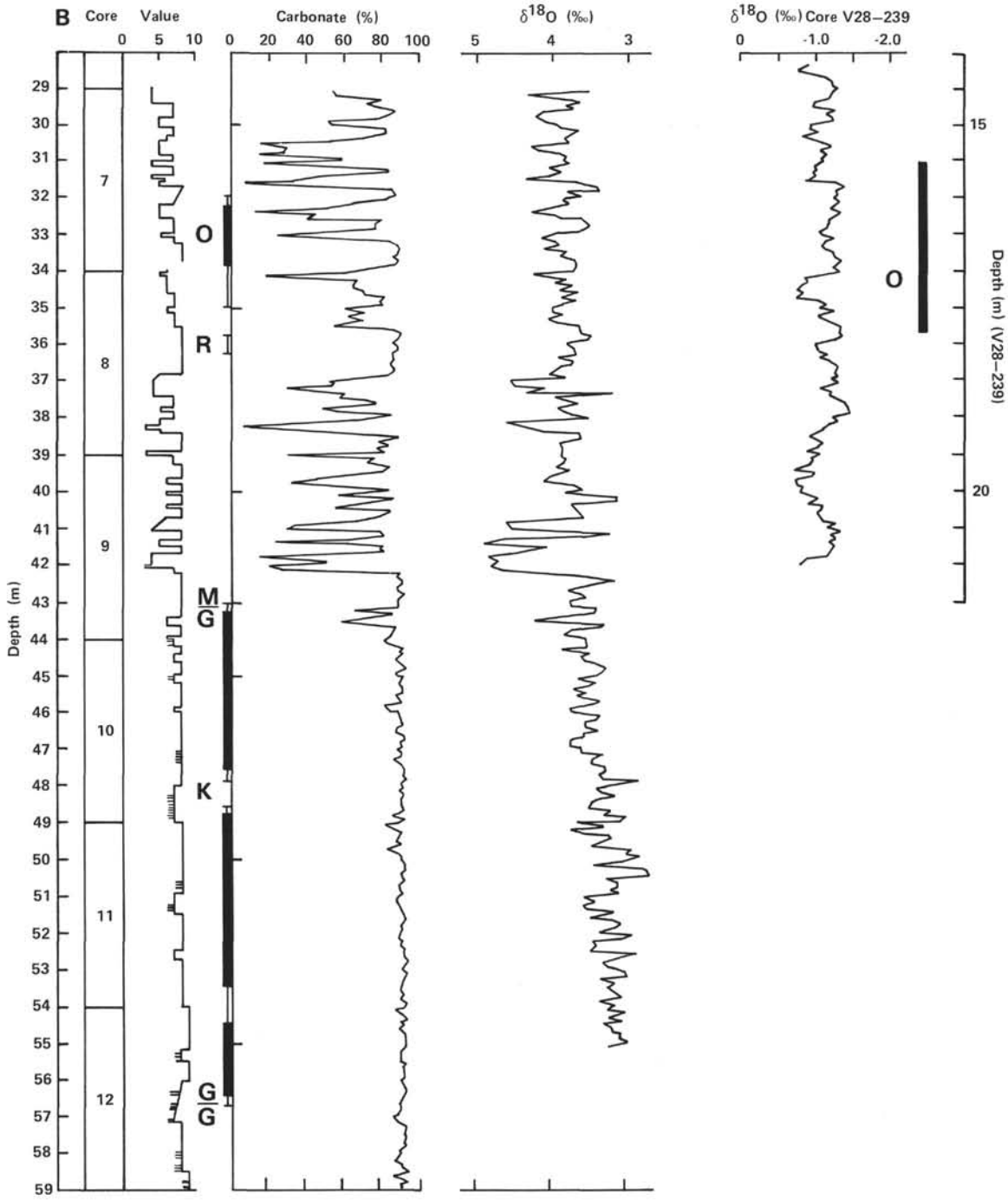

Figure 7. (Continued).

CONCLUSIONS

DSDP Hole 552A was cored with the HPC on Hatton Drift and obtained an almost complete and undisturbed sediment section spanning the late Neogene and Quaternary. Lithologic, faunal, isotopic, and paleomagnetic analyses indicate that the section represents the most complete deep sea record of climatic evolution hitherto recovered in the high latitude northern hemisphere. On the basis of the foregoing studies, the following conclusions seem warranted:

1. The climate–ocean system, expressed as lithologic parameters, clearly shows a cyclic mode of variation. The gross lithology is a sequence of alternating white pelagic-calcareous ooze and dark muds rich in ice-rafted debris. Composition of the acid-insoluble coarse fraction and geographic position of Hole 552A suggest Greenland as the most probable origin of the ice-rafted debris.

2. The cyclic nature of the sediments extends to the included organic material. The glacial muds, with a relatively high content of organic carbon of a reworked character, reflect the lowered sea levels and increased con-

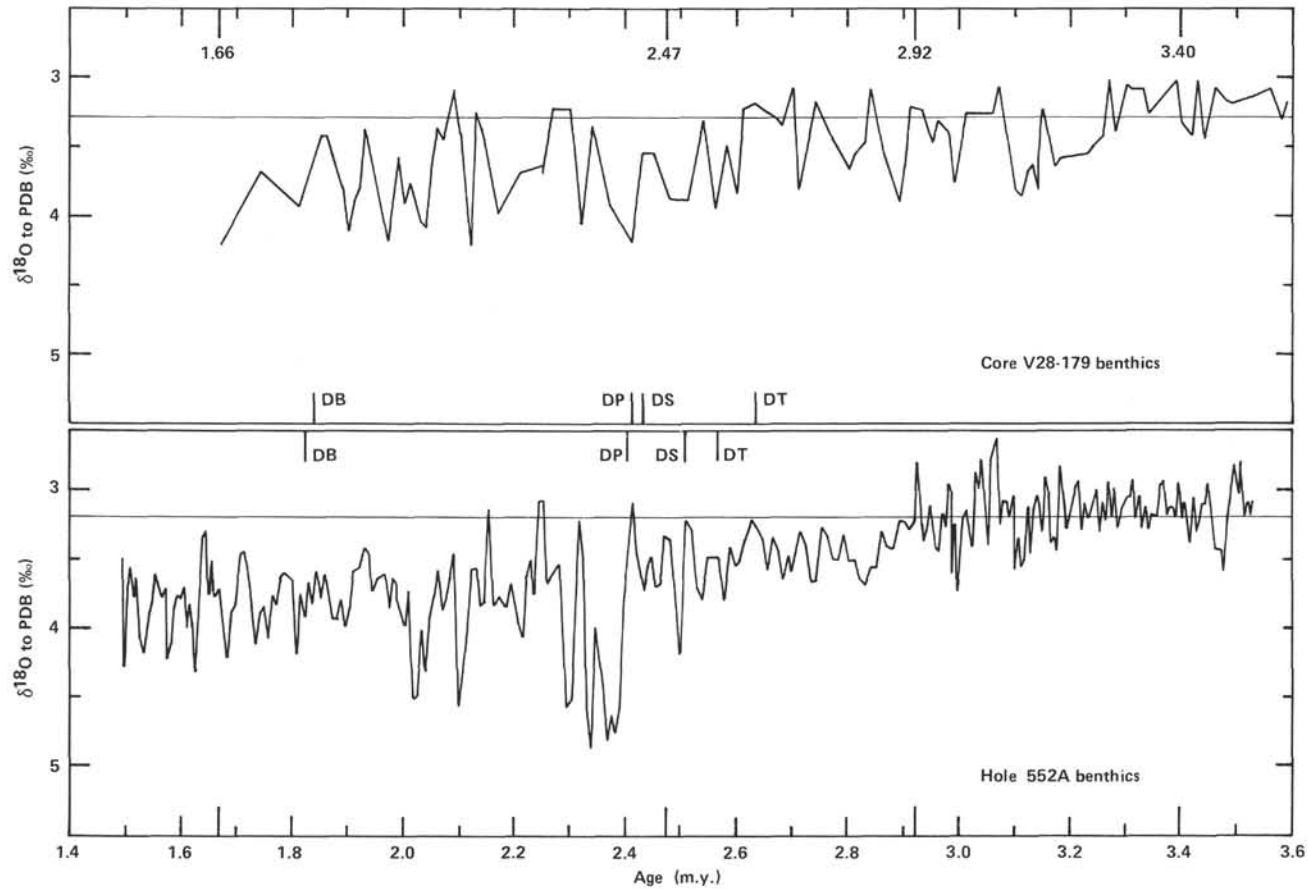

Figure 8. Oxygen isotope data of Hole 552A (Cores 7–12) plotted on an age scale of linear adjustment between magnetic reversals. The oxygen isotope record for Pacific core V28-179 (Shackleton and Opdyke, 1977) is plotted at the same age scale for comparison; time control is shown — 1.66 m.y., top Olduvai N subchron; 2.47 m.y. ago, base Matuyama R chron; 2.92 m.y., top Kaena R subchron; 3.40 m.y., base Gauss N chron. Nannofossil extinction horizons determined for both cores: DT, *Discoaster tamalis*; DS, *D. surculus*; DP, *D. pentaradiatus*; DB, *D. brouweri*. Horizontal lines indicate the present position of O^{18} equilibrium.

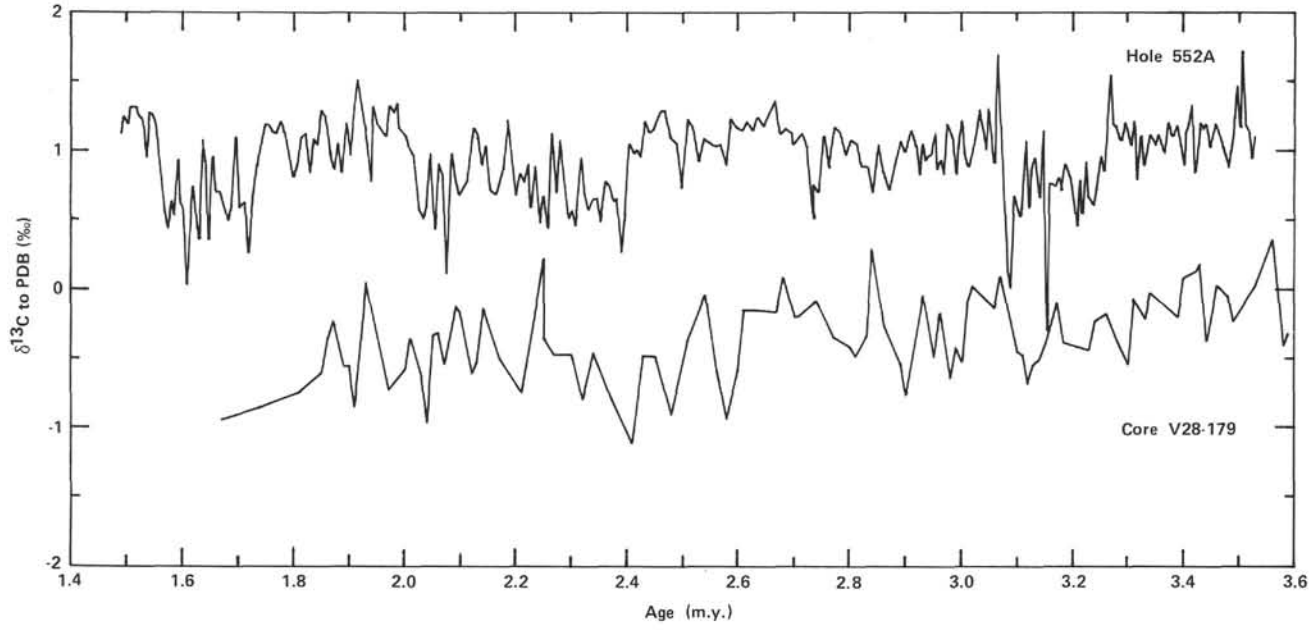

Figure 9. Carbon isotope records for Hole 552A (Cores 7–12) and Pacific core V28-179. Both records are plotted on the same ^{13}C and age scales.

tinental erosion of glacial episodes. The enhanced levels of organic phosphorus in organic material of the interglacial stages suggest a pelagic–marine source.

3. The carbonate and coarse fraction data reflect the variation of the calcareous components produced under the rapidly changing climatic regimes of the past 2.4 m.y. Spikes of low coarse fraction carbonate may indicate particularly intense cold periods with extensive ice cover and resulting low productivity in the northeastern Atlantic. In the opposite sense, episodes of particular warmth are suggested by isolated occurrences of temperate diatoms.

4. In the upper part of the section, DSDP Hole 552A preserves the whole of the standard oxygen isotope record of the past million years. We have extended the isotope stage stratigraphy to interglacial stage 25 which includes the base of the Jaramillo subchron at 0.98 m.y. ago.

5. Oxygen isotope analysis of the sequence together with nannofossil and magnetostratigraphic time control indicate that the first major glacial event, as represented by coincident ice volume and ice-rafting horizons, occurs at 2.37 m.y. ago, well before the Pliocene/Pleistocene boundary. These data do not support the notion of significant northern hemisphere glaciation prior to 2.5 m.y. ago.

6. The carbon isotope record shows that Hole 552A has been bathed by a water mass with characteristics similar to those of present-day North Atlantic Deep Water at least since 3.5 m.y. ago and that quasi-cyclic alternations in the intensity of its production were occurring during the Pliocene prior to the onset of extensive glaciation in the northern hemisphere.

ACKNOWLEDGMENTS

The authors would like to thank the staff at DSDP for the opportunity to participate on Leg 81 and for their encouragement to complete this study. The good fellowship and stimulating collaboration of the shipboard scientific party will serve as a model for future cruises. Our sincere thanks to the captain and crew of The D/V *Glomar Challenger* for a job well done under the trying circumstances of the North Atlantic.

REFERENCES

Backman, J., 1979. Pliocene biostratigraphy of DSDP Sites 111 and 116 from the North Atlantic Ocean and the age of northern hemisphere glaciation. *Stockholm Contrib. Geol.*, 32:113–137.

Backman, J., and Shackleton, N. J., 1983. Quantitative biochronology of Pliocene and early Pleistocene calcareous nannofossils from the Atlantic, Indian and Pacific Oceans. *Mar. Micropaleontol.*, 8: 141–170.

Backman, J., Shackleton, J. J. and Tauxe, L., 1983. Quantitative nannofossil correlation to open ocean deep sea sections from the Plio-Pleistocene boundary at Vrica, Italy. *Nature*, 304:156–158.

Berggren, W. A., 1972. Late Pliocene–Pleistocene glaciation. *In* Laughton, A. S., Berggren, W. A., et al., *Init. Repts. DSDP*, 12: Washington (U.S. Govt. Printing Office), 953–963.

Berggren, W. A., Kent, D. V., and Van Couvering, J., in press. Neogene geochronology and chronostratigraphy. *J. Geol. Soc. London.*

Donn, W. L., and Ninkovitch, D., 1980. Rate of Cenozoic explosive volcanism in the North Atlantic Ocean inferred from deep sea cores. *J. Geophys. Res.*, 85:5455–5460.

Goree, W. S., and Fuller, M., 1976. Magnetometers using RF-driven squids and their application in rock magnetism and paleomagnetism. *Rev. Geophys. Space Phys.*, 14:591–608.

Harrison, R. K., Knox, R. W. O'B., and Morton, A. C., 1979. Petrography and mineralogy of volcanogenic sediments from DSDP Leg 48, southwest Rockall Plateau, Site 403 and 404. *In* Montadert, L., Roberts, D. G., et al., *Init. Repts. DSDP*, 48: Washington (U.S. Govt. Printing Office), 771–785.

Heiken, G., 1975. An atlas of volcanic ash. *Smithsonian Contrib. Earth Sci.*, 12:1–101.

Hodell, D. A., Kennett, J. P., and Leonard, K. A., 1983. Climatically induced changes in vertical water mass structure of the Vema Channel: Evidence from Deep Sea Drilling Project Holes 516A, 517, and 518. *In* Barker, P. F., Johnson, D. A., et al., *Init. Repts. DSDP*, 72: Washington (U.S. Govt. Printing Office), 907–920.

Hodell, D. A., Williams, D. F., and Kennett, J. P., in press. Reorganization of deep vertical water mass structure in Vema Channel at 3.2 Ma: faunal and isotopic evidence from DSDP Leg 72. *Geol. Soc. Am. Bull.*

Kroopnick, P., 1980. The distribution of ^{13}C in the Atlantic Ocean. *Earth Planet. Sci Lett.*, 49:469–484.

McCave, I. N., Lonsdale, P. F., Hollister, C. D., and Gardner, W. D., 1980. Sediment transport over the Hatton and Gardar Contourite Drifts. *J. Sediment, Petrol.*, 50:1049–1062.

Müller, G., and Gastner, M., 1971. The "Karbonate-Bombe," a simple device for the determination of the carbonate content in sediments, soils, and other materials. *N. Jb. Miner, Mh.*, 10:466–469.

Poore, R. Z., 1981. Temporal and spatial distribution of ice-rafted mineral grains in Pliocene sediments of the North Atlantic: Implications for late Cenozoic climatic history. *SEPM Spec. Publ.*, 32: 505–515.

Prell, W. L., 1982. A reevaluation of the initiation of northern hemisphere glaciation at 3.2 m.y.: New isotope evidence. *Geol. Soc. Am.*, (95th Ann. Mtg.), p. 592 (Abstract with program).

Ruddiman, W. F., and Glover, L. K., 1972. Vertical mixing of ice-rafted volcanic ash in North Atlantic sediments. *Geol. Soc. Am. Bull.*, 83:2817–2836.

Ruddiman, W. F., and McIntyre, A., 1976. Northeast Atlantic paleoclimatic changes over the past 600,000 years. *Mem. Geol. Soc. Am.*, 145:111–146.

Schrader, H. J., and Fenner, J., 1976. Norwegian diatom biostratigraphy and taxonomy. *In* Talwani, M., Udintsev., G., et al., *Init Repts. DSDP*, 38: Washington (U.S. Govt. Printing Office), 921–1098.

Shackleton, N. J., Backman, J., Zimmermann, H. B., Kent, D. V., Hall, M. A., Roberts, D. G., Schnitker, D., Baldauf, J. G., Desprairies, A., Homrighausen, R., Huddlestun, P., Keene, J. B., Kaltenback, A. J., Krumsiek, K. A. O., Morton, A. C., Murray, J. W., and Westberg-Smith, J., 1984. Oxygen isotope calibration of the onset of icerafting in DSDP Site 552A: History of glaciation in the North Atlantic region. *Nature*, 307:620–623.

Shackleton, N. J., and Opdyke, N. D., 1973. Oxygen isotope and paleomagnetic stratigraphy of equatorial Pacific core V28-238: Oxygen isotope temperatures and ice volumes on a 10^5 year and 10^6 year scale. *Quat. Res.*, 3:39–55.

_____, 1976. Oxygen-isotope and paleomagnetic stratigraphy of Pacific core V28-239, late Pliocene to latest Pleistocene. *Mem. Geol. Soc. Am.*, 145:449–464.

_____, 1977. Oxygen isotope and paleomagnetic evidence for early Northern Hemisphere glaciation. *Nature*, 270: 216–219.

Sylvester, A. G., 1976. Petrography of volcanic ashes in deep-sea cores near Jan-Mayen Island: Sites 338, 345–350, DSDP Leg 38. *In* Talwani, M., Udintsev, G., *Init. Repts. DSDP*, Suppl. to Vols. 38, 39, 40, and 41: Washington (U.S. Govt. Printing Office), 101–106.

Date of Acceptance: January 30, 1984